Available online at www.sciencedirect.com
ScienceDirect
Trans. Nonferrous Met. Soc. China 20(2010) s648−s654
Transactions of Nonferrous Metals Society of China
www.tnmsc.cn

Preparation and characterization of Ca-P coating on AZ31 magnesium alloy

TAN Li-li(谭丽丽)[1], WANG Qiang(王 强)[1, 2], GENG Fang(耿 芳)[1], XI Xiao-song(席小松)[3], QIU Jian-hong(邱剑红)[3], YANG Ke(杨 柯)[1]

1. Institute of Metal Research, Chinese Academy of Sciences, Shenyang 110016, China;
2. School of Stomatology, China Medical University, Shenyang 110002, China;
3. Trauson Medical Instrument Co., Ltd., Changzhou 213163, China

Received 23 September 2009; accepted 30 January 2010

Abstract: A Ca-P coating consisting of biodegradable β-tricalcium phosphate [β-TCP, β-$Ca_3(PO_4)_2$] accepted for medical application was coated on a biodegradable AZ31 alloy by chemical deposition to improve the corrosion resistance. The good bonding strength of the coating is obtained. The results show that the corrosion potential of the Ca-P coated AZ31 alloy increases significantly, and MG63 cells show good adherence, proliferation and differentiation on the surface of the coated alloy. The Ca-P coating might be an effective way to improve the surface bioactivity of magnesium alloys.
Key words: biodegradable magnesium alloy; β-TCP; chemical deposition; biocompatibility

1 Introduction

Magnesium (Mg) alloys has attracted much attention as potential biodegradable bone implant materials due to their biodegradability and non-toxicity to the human body[1−2]. However, the surface treatment is necessary to protect against the severe corrosion because Mg is a considerably active metal in chloride contained solutions including human body fluid or blood plasma[3−4]. The high hemolytic rate is accompanied with Mg and its alloys due to their rapid corrosion. Though several new Mg alloys were developed to solve this problem, they still cannot well match the hemolysis requirement of lower than 5% without surface treatment.

Up to now, there are some surface techniques to improve the corrosion resistance of Mg alloy exposed to physiological environment. The typical surface coatings include TiN, CrN, AlN, Ti-Al-N and TiO_2[5−9]. The nitrogen plasma ion implantation was reported to be effective to improve the corrosion resistance of Mg alloy under proper conditions[10]. The oxide coatings were produced on AM60B alloy substrate by microarc oxidation (MAO) technique in alkali electrolytic solution[11]. A thick and porous layer composed of MgO and MgF_2 was also prepared on pure Mg using microarc oxidation[12]. However, these coatings still need further confirmation for application on bio-absorbable implant materials.

Bioactive Ca-P coating on Mg alloys might be a way to overcome the above problem. It was reported that anodization could be used to fabricate a calcium phosphate film on pure magnesium[13] and a porous and netlike $CaHPO_4{\cdot}2H_2O$ layer was coated on the surface of the Mg-Mn-Zn alloy[14]. The chemical deposition, a low temperature route, was one of simple methods used for surface modification of biomaterials. The alkali-heat treatment method could induce a biomimetic precipitation of calcium phosphate on the implant surface[15]. A porous and netlike $CaHPO_4{\cdot}2H_2O$ layer could be formed on the surface of the Mg-Mn-Zn alloy[16]. The bioactivity of the Ca-P coating was evaluated in detail and the researcher suggested that the Ca-P coating should be an effective way to improve the surface bioactivity of Mg alloy. β-TCP coating has been proved to be degradable in physiological environment and to show good early interaction between the implant and the tissue. However, the preparation and effect of β-TCP coating on biodegradable AZ31 magnesium alloy has less been reported.

Foundation item: Project(KGCX2-YW-207) supported by Chinese Academy of Sciences, China; Project(30970715) supported by National Natural Science Foundation of China
Corresponding author: YANG Ke; Tel: +86-24-23971628; E-mail: kyang@imr.ac.cn

In the present study, a biodegradable Ca-P coating mainly consisting of β-TCP and $CaPO_3(OH)$ was fabricated on AZ31 magnesium alloy via chemical deposition. The microstructure and composition of the coating were characterized. The bonding strength, corrosion, behavior and bioactivity including cell culture, alkaline phosphatase (ALP) activity and hemolytic ratio were also studied.

2 Experimental

2.1 Preparation of Ca-P coating

An extruded AZ31 Mg alloy with nominal composition of Mg-3%Al-1%Zn was cut into 10 mm×10 mm×2 mm pieces samples, ground, polished with SiC papers to 1 200 grits, ultrasonically rinsed in alcohol for 10 min in alcohol and finally dried. Then, the samples were immersed in Na_2HPO_4 solution at 60 ˚C and ultrasonically cleaned again in distilled water. After the above treatment, the samples were immersed in the solution of $NaH_2PO_4·12H_2O$ and $Ca(NO_3)_2$ at 70 ˚C for 48 h. The samples were then washed with distilled water and dried in air. The microstructures of the Ca-P coated samples were observed on an S−3400N scanning electronic microscope (SEM) coupled with energy dispersive spectrometer (EDS). The phase composition was characterized by an X-ray diffractometer (Philips PW1700) using Cu K_α.

2.2 Bonding strength test

The bonding strength of the Ca-P coating with the AZ31 substrate was measured using an AG-100kNG mechanical testing machine. Two coated samples were bonded together with epoxy resin. After two days stabilization, the bonding strength test was carried out with loading rate of 1 mm/min. The testing equipment is schematically shown in Fig.1. The bonding strength is obtained from the recorded maximum load.

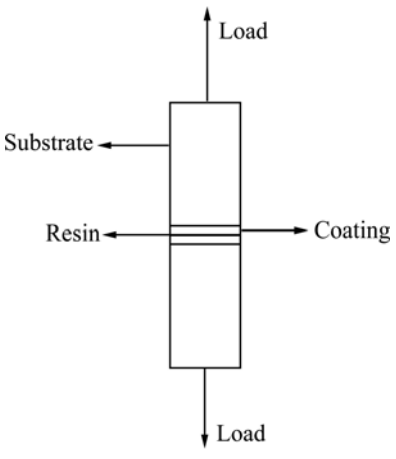

Fig.1 Schematic diagram of bonding strength test of Ca-P coating on AZ31B alloy

2.3 Electrochemical experiments

The electrochemical experiments including potentiodynamic polarization and electrochemical impedance spectroscopy (EIS) were performed using a model 273 EG&G PARC Potentiostat-Galvanostat in an electrolytic solutions of simulated human body fluid (Hank's solution). The composition of Hank's solution is as follows: NaCl 8 g/L, KCl 0.40 g/L, $MgSO_4·7H_2O$ 0.10 g/L, $MgCl_2·6H_2O$ 0.10 g/L, $CaCl_2$ 0.14 g/L, $Na_2HPO_4·2H_2O$ 0.06 g/L, KH_2PO_4 0.06 g/L and glucose 1 g/L. The experimental set-up consists of a conventional three-electrode cell containing a working electrode, a saturated calomel electrode (SCE) and a platinum sheet as the counter electrode. As for the potentiodynamic polarization measurement, the scan was started from 250 mV below the anode corrosion potential at scanning rate of 0.5 mV/s. The EIS measurement was made using a lock-in amplifier (Model 5210, EG & Instrument) coupled with a Potentiostat-Galvanostat system. EIS spectra were obtained at the open-circuit potential of the specimens in Hank's solution with an amplitude of 5 mV. The frequency span is 10^{-2}−10^5 Hz. The data registration and analysis were performed on an interfaced computer. The analysis of the spectra was performed with Z-View2 software for convenience.

2.4 Cytocompatibility test

2.4.1 Live and dead staining and SEM observation

Human osteoblast-like cells MG63 widely used to investigate the adhesion, proliferation and differentiation of bone cells were cultured in DMEM medium containing 7% FBS at 37 ˚C in 5% CO_2 humidified atmosphere and then were used for cytocompatibility tests. The cells MG63 were seeded on the Ca-P coated AZ31 samples at a cell density of $1×10^6$ mL^{-1}. After separated incubation in a 24-well microplate for 48 h, the samples were washed for three times with PBS to remove the non-adherent cells. The living and dead cells adhered on the samples were stained with AO–EB, and then visualized using a Leica DMLB fluorescence microscope. After incubations for 4, 7 and 10 d, the ALP activities of the cells on the samples were measured, with 3 wells for each material at each time, using a method adapted by BORSARI et al[17].

2.4.2 Hemolysis test

Samples with dimensions of 11 mm×11 mm×3 mm were used for the hemolysis test. 2.5 mL normal saline as the negative control, 2.5 mL distilled water as the positive control, and three tested samples in 2.5 mL normal saline were incubated in tubes at 37 ˚C for 30 min. Then, 70 μL diluted human blood was added into each tube. The tubes were gently shaken, incubated at 37 ˚C for 60 min and centrifuged at 3 500 r/min for

5 min. The optical density of the supernatant liquor was measured in absorbance at wavelength of 545 nm by a spectrophotometer (GF−M2000 Microplate Reader, China). The hemolytic ratio (H) was obtained by the following equation:

$$H=(D_t-D_{nc})/(D_{pc}-D_{nc})\times 100\%$$

where D_t is the absorbance of the testing sample; D_{pc} and D_{nc} are the absorbances of the positive and negative control group, respectively.

3 Results and analysis

3.1 Surface microstructure and composition of Ca-P coating on AZ31 alloy

Fig.2(a) shows the surface morphology and structure of the as-deposited coating. It can be seen from Fig.2(a) that the surface coating mainly exhibits regular flower-like structure diverging from the center toward the periphery. Fig.2(b) indicates that the Ca-P coating with thickness of about 15−20 μm is bonded well with the AZ31 substrate. The line-scan analysis confirms that the fabricated coating mainly consists of Ca, P and O elements. The XRD result, as shown in Fig.2(c), shows that the as-deposited coating mainly consists of [β-TCP, β-$Ca_3(PO_4)_2$] and calcium phosphate ($CaPO_3(OH)$). The average bonding strength between the Ca-P coating and the AZ31 substrate is higher than 20.2 MPa, as shown in Fig.3(a). SEM observation on the Ca-P coated surface after adhesion test shows that the Ca-P coating is not peeled off at the failure point, as shown in Fig.3(b).

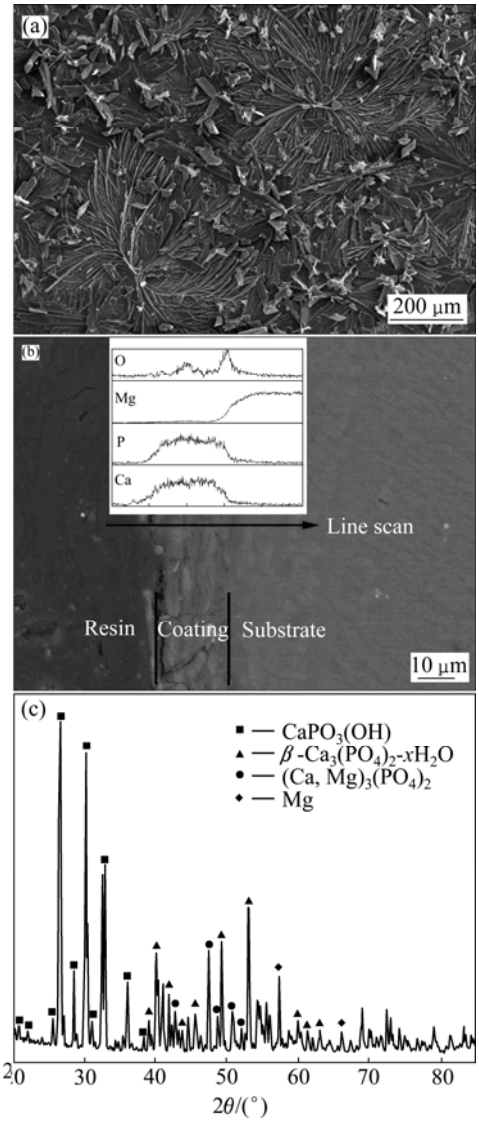

Fig.2 Morphologies of surface (a) and cross section (b) and XRD pattern (c) of as-deposited coating on AZ31 alloy

3.2 Electrochemical measurement

The potentiodynamic polarization curves of the Ca-P coated AZ31 alloy samples in Hank's solution at (37±1) ˚C are shown in Fig.4 and the fitting results are shown in Table 1. The current density of all the Ca-P

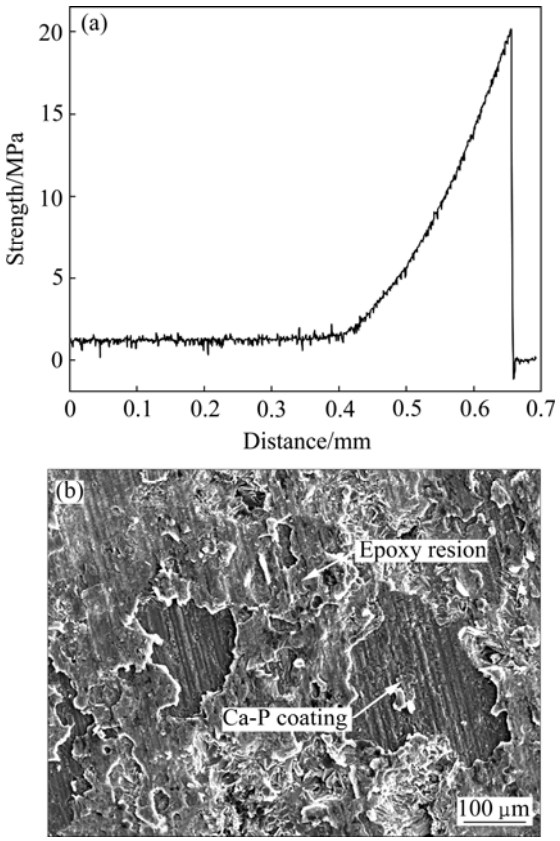

Fig.3 Tensile curve(a) and fracture morphology(b) of Ca-P coated surface on AZ31 alloy after adhesion test

Table 1 Fitting results of polarization curves for naked and Ca-P coated AZ31 alloys

Material	φ_{corr}/ V	φ_b/ V	J_{corr}/ (10^{-6} A·cm^{-2})	J_b/ (10^{-6} A·cm^{-2})
Naked AZ31 alloy	−1.607	−	293.0	−
Ca-P coated AZ31 alloy	−1.483	−1.41	2.346	7.088

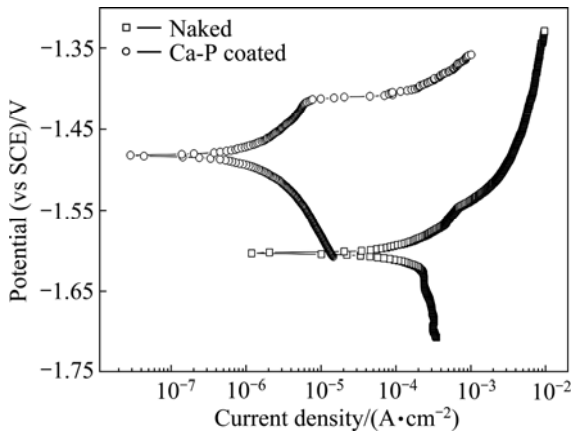

Fig.4 Potentiodynamic polarization curves of naked and Ca-P coated AZ31 alloys

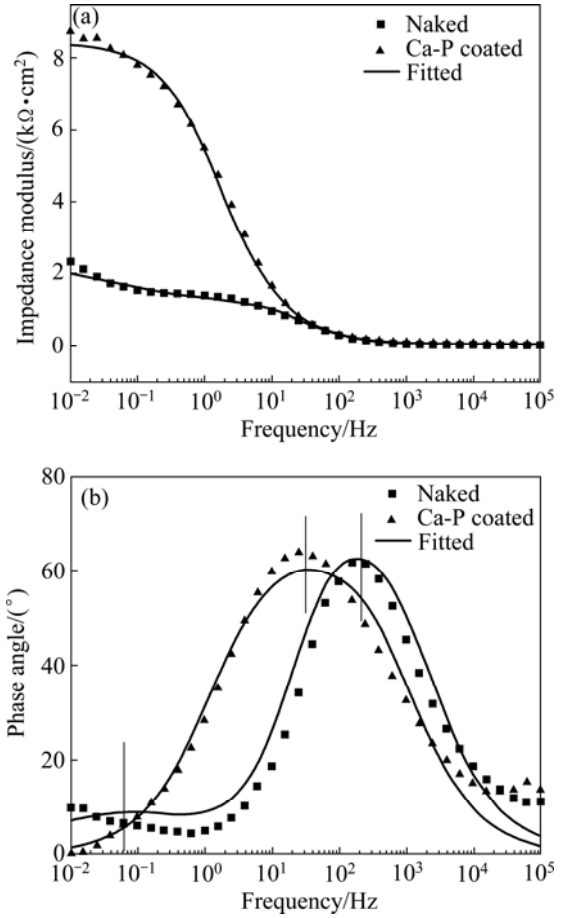

Fig.5 Experimental and fitting EIS spectra of naked and Ca-P coated AZ31 alloys

coated AZ31 samples decreases, while the corrosion potential (φ_{corr}) and breakdown potential (φ_b) of the sample increase significantly compared with those of the naked AZ31 sample.

EIS spectra and the corresponding fitting results of the samples measured in Hank's solution are shown in Fig.5, with the impedance modulus and the phase angle plotted versus frequency. The electrical equivalent circuits are presented in Fig.6 according to the measured spectra. It can be found that there is good conformity between the experimental and theoretical spectra. In general, the CPE is given as both the capacitance C and the factor n ($0 \leq n \leq 1$)[18]. R_s is the resistance of the electrolyte. For the naked AZ31 alloy, R_p is the resistance of the oxide layer and R_t represents the difficulty degree of the substrate oxidation. C_p and C_t are the capacitance parameters of the electrolyte/oxide and oxide/substrate interfaces. For the coated AZ31 samples, R_p is the polarization resistance and C_p is the interface capacitance. The determined values of the electrical elements are shown in Table 2. The R_p of the coating and substrate are 1 110 Ω·cm^2 and 8 399 Ω·cm^2, respectively. The R_t of the substrate is about 1 384 Ω·cm^2. The C_p values for both the coating and substrate are in the same order of magnitude. However, C_t for the substrate is 1 627 mF/cm^2. Higher R_p and lower C_p mean better corrosion resistance.

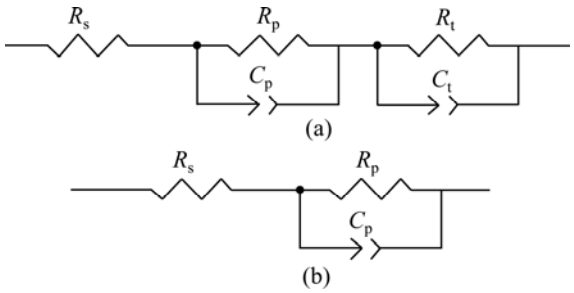

Fig.6 Electrical equivalent circuits of EIS spectra for naked (a) and Ca-P coated (b) AZ31 alloys

Table 2 EIS spectra fitting results for naked and Ca-P coated AZ31 alloys

Material	R_p/ (Ω·cm^{-2})	C_p/ (10^{-5} F·cm^{-2})	R_t/ (Ω·cm^{-2})	C_t/ (10^{-5} F·cm^{-2})
Naked AZ31 alloy	1 110	1.186	1 384	162.7
Ca-P coated AZ31 alloy	8 399	2.591	–	–

3.3 Biocompatibility

After 48 h incubation with cells, the fluorescence photo shows adhesions of many viable MG63 cells on the Ca-P coated AZ31 Mg alloy, which means that the surface modified sample has good affinity to cells, as shown in Fig.7. The living and dead cells are stained, respectively, with AO-EB and visualized in green and red under a fluorescence microscopy. This indicates that the Ca-P coated AZ31 alloy is compatible for bone growth at the early healing process. However, no MG63 cell is found on the naked AZ31 samples.

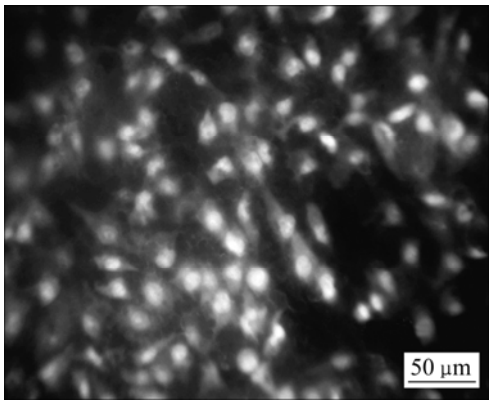

Fig.7 Fluorescence micrographs of living and dead dye-stained MG63 cells cultured on Ca-P coated AZ31 alloy for 48 h

Alkaline phosphatase is a specific enzyme made in liver, bone and the placenta of human body, and is normally present in high concentration in growing bones. The osteoblast differentiation generally implies the ALP activity[19]. The ALP activities of MG63 cells in the experimental and control groups at various time points are shown in Fig.8. It is found that ALP activity increases obviously with increasing the culturing time in both groups. However, the cells on the coated samples proliferate much more and express higher ALP levels compared to those on the naked sample, which indicates the improvement on bone growth by coating.

Fig.9 shows the hemolytic ratio of the coated and naked AZ31 samples. From Fig.9, the hemolytic ratio of the naked AZ31 sample is about 90%, much higher than 5% that is the safe limit for implanted biomaterials according with ISO standard 10993-4, indicating that the naked AZ31 can cause severe hemolysis if being contacted with blood. However, the hemolysis of the coated sample is only about 4.3%, indicating that the Ca-P coating can greatly improve the biocompatibility of AZ31 alloy.

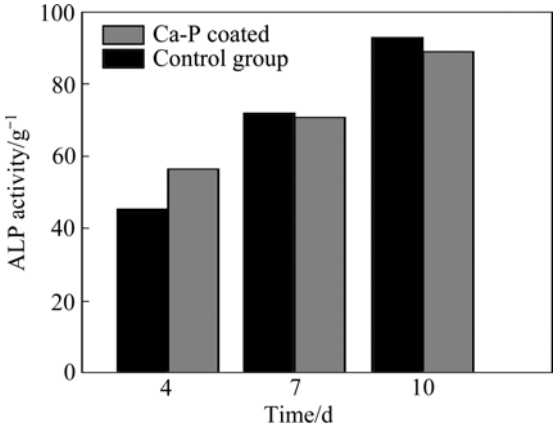

Fig.8 ALP activities of MG63 cells on Ca-P coated AZ31 and control samples at various times

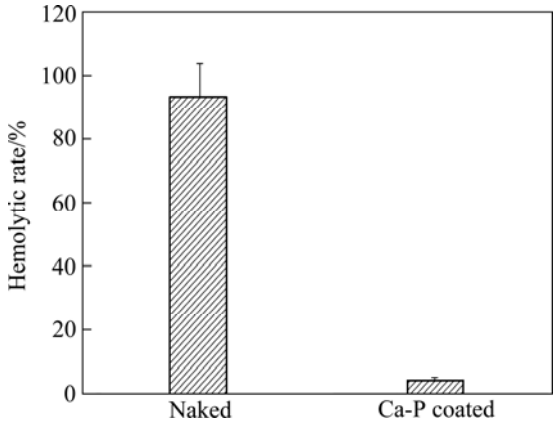

Fig.9 Hemolysis rate of naked and Ca-P coated AZ31 alloys

4 Discussion

The Ca-P coating mainly consisting of β-TCP on AZ31 magnesium alloy was investigated in the present work in order to decrease the degradation rate and improve the biocompatibility of AZ31 alloy. The Ca-P coating is well deposited on AZ31 alloy via a low temperature method and the surface structure shows the compact and uniform coating. The EDS analysis indicates that the coating is mainly composed of Ca, P, O and Mg elements, and the main phase constituents are β-TCP and $CaPO_3(OH)$. The average bonding strength between the Ca-P coating and AZ31 substrate is measured to be more than 20.2 MPa because the coating cannot be peeled off when the loading reaches the critical point. The interfacial bonding strengths between different metal substrates and Ca-P coating were generally reported in a range of 12−65 MPa. For instances, the mean bonding strength of plasma-sprayed hydroxyapatite coating on titanium alloys is in the range of 12.9−17.3 MPa[20], and the bonding strength of HA/TiO_2 double layer coating fabricated by different ways on titanium substrate is 20−60 MPa[21]. KUMAR and MARUNO[22] reported that the bonding strength between the HA-G-Ti composite and the bone was 2.7−20.6 MPa. In general, the better adhesion strength is believed to come from an enhanced chemical bonding between the Ca-P coating and the substrate.

The corrosion of Mg alloys has been a major obstacle to their development for biomedical applications[23]. From the electrochemical experimental result, it can be seen that the current density of the naked AZ31 sample increases significantly with increasing the potential because the loose oxide film formed on the surface cannot well protect the alloy from corrosion. The pitting corrosion is not obvious on the surface, which means that only uniform corrosion happens. However, it can be seen that the Ca-P coating can effectively inhibit

the corrosion of the substrate and the breakdown potential is increased to −1.41 V, above which the pitting corrosion happens. The anodic current density of the coated samples is lower than that of the naked sample at the same potential. According to the principle of corrosion electrochemistry, the corrosion rate is proportional to the anodic current density.

EIS spectra further illustrate the above point. As shown in Fig.5, two time constants of the naked alloy are generally observed because of the presence of the passive layer on the electrode surface. The time constant at the higher frequency should be attributed to the formation of the oxide layer and the second constant to the metal/oxide interface where the electrochemical oxidation on the metal occurs. However, EIS spectra of the Ca-P coated samples only exhibite one time constant impedance behavior, which indicates that the surface of the substrate has been completely covered by a Ca-P coating. For both types of samples, the impedance modulus at different frequencies can be directly observed from the spectra, and the capacitive behavior is indicated by increasing the impedance with decreasing frequency. In the high frequency region, the impedance is independent of frequency, which is the resistance of the electrolyte between the sample and the reference electrode. At the low frequency limit, the impedance is attributed to the polarization resistance of the sample in the electrolyte. As shown in Table 2, an increase of impedance implies the decrease of degradation rate. C_t of the substrate is much higher than C_p, which indicates that the electrolyte has penetrated the loose oxide layer and accelerated the corrosion of the substrate. The above results confirm the effective protection effect by the Ca-P coating, i.e. the Ca-P coating can effectively reduce the degradation rate of AZ31 alloy. A delayed degradation process is critical to the biodegradable implant, as the implant needs to fully play the function for a certain period of time before the surgery region is healed[4].

The biological properties of the coated samples are assessed in terms of proliferation and differentiation behaviors by means of osteoblast-like MG63 cells, hemolytic ratio and ALP activity. The cells on the coated AZ31 alloy substrate proliferate more actively and express ALP activity to a higher degree, as compared with those on the naked AZ31 alloy. This higher ALP expression on the Ca-P coating system confirms the enhancement of cell function of the material. The creation of a rough and biocompatible surface can also lead to the increase of ALP activity[24]. The hemolysis rate of the naked AZ31 alloy substrate reaches above 90%, which should be caused by the rapid corrosion of the alloy leading to the increase of the pH value in the solution. It was reported that metal ions, such as Al, Zn and Mn, may lead to hemolysis when their concentration reach the critical hemolytic points[25−26]. As the β-CP coating can effectively slow down the degradation of the Mg alloy substrate, the hemolysis of the alloy is then reduced. The above improvements can make the enhancement of biocompatibility for Mg alloys at least at the early stage of implantation. Actually, it was reported that the Ca-P coating containing β-TCP, HA and other calcium and phosphorus compounds is effective to enhance the bioactivity of biomaterials such as titanium alloy and stainless steel etc[21, 27−28]. The present preliminary in vitro studies demonstrates that a chemically deposited Ca-P coating consisting of β-TCP and $CaPO_3(OH)$ can effectively improve the biocompatibility of biodegradable AZ31 magnesium alloy.

5 Conclusions

A protective Ca-P coating with suitable bonding strength has been fabricated on a biodegradable AZ31 magnesium alloy by chemical deposition. The corrosion potential and breakdown potential of the coated AZ31 alloy are obviously enhanced, and the J_{corr} of the coated AZ31 alloy is significantly decreased. The electrochemical impedance measurement demonstrates that the Ca-P coating can lead to significant increase in the polarization resistance and decrease in the interfacial capacitance, i.e. the Ca-P coating can provide a good protection from corrosion for AZ31 alloy, which is important for reduction of the degradation rate in implantation and improvement of the biocompatibility of the alloy. The vitro experiments further demonstrate that the deposited Ca-P coating on AZ31 alloy is beneficial to blood biocompatibility and growth of bones.

References

[1] WITTE F, KAESE V, HAFERKAMP H, SWITZER E, MEYER-LINDENBERG A, WIRTH C J, WINDHAGEN H. In vivo corrosion of four magnesium alloys and the associated bone response [J]. Biomaterials, 2005, 26(17): 3557−3563.

[2] XU L, YU G, ZHANG E, PAN F, YANG K. In vivo corrosion behavior of Mg-Mn-Zn alloy for bone implant application [J]. J Biomed Mater Res, 2007, 83A: 703−711.

[3] STAIGER M P, PIETAK A M, HUADMAI J, DIAS G. Magnesium and its alloys as orthopedic biomaterials: A review [J]. Biomaterials, 2006, 27(9): 1728−1734.

[4] SONG Guang-ling. Control of biodegradation of biocompatable magnesium alloys [J]. Corrosion Science, 2007, 49(4): 1696−1701.

[5] WU Guo-song, WANG Xue-min, DING Ke-jian, ZHOU Yuan-yuan, ZENG Xiao-qin. Corrosion behavior of Ti-Al-N/Ti-Al duplex coating on AZ31 magnesium alloy in NaCl aqueous solution [J]. Materials Characterization, 2009, 60(8): 803−807.

[6] ZENG X, WU G, YAO S. Formation by reactive magnetron sputtering of TiN coating on Ti-implanted magnesium alloy [J]. Materials Letters, 2006, 60(17/18): 2252−2255.

[7] HOCHE H, ROSENKRANZ C, DELP A. Investigation of the macroscopic and microscopic electrochemical corrosion behaviour of PVD-coated magnesium die cast alloy AZ91 [J]. Surf Coat Technol, 2005, 193(1/3): 178−184.

[8] HU Jun-hua, GUAN Shao-kang, ZHANG Cai-li, REN Chen-xing, WEN Cui-lian, ZENG Zhao-qin, PENG Li. Corrosion protection of AZ31 magnesium alloy by a TiO_2 coating prepared by LPD method [J]. Surf Coat Technol, 2009, 203(14): 2017−2020.

[9] ALTUN H, SEN S. The effect of PVD coatings on the wear behaviour of magnesium alloys [J]. Materials Characterization, 2007, 58(10): 917−921.

[10] TIAN X B, WEI C B, YANG S Q, FU R K Y, CHU P K. Corrosion resistance improvement of magnesium alloy using nitrogen plasma ion implantation [J]. Surf Coat Technol, 2005, 198(1/3): 454−458.

[11] LIANG J, GUO B, TIAN J, LIU H, ZHOU J, XU T. Effect of potassium fluoride in electrolytic solution on the structure and properties of microarc oxidation coatings on magnesium alloy [J]. Applied Surface Science, 2005, 252(2): 345−351.

[12] SHI P, NG W F, WONG M H, CHENG F T. Improvement of corrosion resistance of pure magnesium in Hanks' solution by microarc oxidation with sol-gel TiO_2 sealing [J]. Journal of Alloys and Compounds, 2009, 469(1/2): 286−292.

[13] HIROMOTO S, SHISHIDO T, YAMAMOTO A, MARUYAMA N, SOMEKAWA H, MUKAI T. Precipitation control of calcium phosphate on pure magnesium by anodization [J]. Corrosion Science, 2008, 50(10): 2906−2913.

[14] SONG Y W, SHAN D Y, HAN E H. Electrodeposition of hydroxyapatite coating on AZ91D magnesium alloy for biomaterial application [J]. Materials Letters, 2008, 62(17/18): 3276−3279.

[15] LI L C, GAO J C, WANG Y. Evaluation of cyto-toxicity and corrosion behavior of alkali-heat-treated magnesium in simulated body fluid [J]. Surf Coat Technol, 2004, 185(1): 92−98.

[16] XU Li-ping, PAN Feng, YU Guo-ning, YANG Lei, ZHANG Er-lin, YANG Ke. In vitro and in vivo evaluation of the surface bioactivity of a calcium phosphate coated magnesium alloy [J]. Biomaterials, 2009, 30(8): 1512−1523.

[17] BORSARI V, GIAVARESI G, FINI M, TORRICELLI P, TSCHON M, CHIESA R, et al. Comparative in vitro study on a ultra-high roughness and dense titanium coating [J]. Biomaterials, 2005, 26(24): 4948−4955.

[18] SONG H K, HWANG H Y, LEE K H, DAO L H. The effect of pore size distribution on the frequency dispersion of porous electrodes [J]. Electrochimica Acta, 2000, 45(14): 2241−2257.

[19] ANSELME K. Osteoblast adhesion on biomaterials [J]. Biomaterials, 2000, 21(7): 667−681.

[20] ZHENG Xue-bin, HUANG Min-hui, DING Chuan-xian. Bond strength of plasma-sprayed hydroxyapatite/Ti composite coatings [J]. Biomaterials, 2000, 21(8): 841−849.

[21] KIM H W, KOH Y H, LI L H, LEE S, KIM H E. Hydroxyapatite coating on titanium substrate with titania buffer layer processed by sol-gel method [J]. Biomaterials, 2004, 25(13): 2533−2538.

[22] KUMAR R R, MARUNO S. Functionally graded coatings of HA-G-Ti composites and their in vivo studies [J]. Mater Sci Eng A, 2002, 334(1/2): 156−162.

[23] PARDO A, MERINO M C, COY A E, ARRABAL R, VIEJO F, MATYKINA E. Corrosion behaviour of magnesium/aluminium alloys in 3.5 wt.% NaCl [J]. Corrosion Science, 2008, 50(3): 823−834.

[24] LI L H, KIM H W, LEE S H, KONG Y M, KIM H E. Biocompatibility of titanium implants modified by micro arc oxidation and hydroxyapatite coating [J]. J Biomed Mater Res Part A, 2005, 73(1): 48−54.

[25] GU Xue-nan, ZHENG Yu-feng, CHENG Yan, ZHONG Sheng-ping, XI Ting-fei. In vitro corrosion and biocompatibility of binary magnesium alloys [J]. Biomaterials, 2009, 30(4): 484−498.

[26] ZHANG Er-lin, YIN Dong-song, XU Li-ping, YANG Lei, YANG Ke. Microstructure, mechanical and corrosion properties and biocompatibility of Mg-Zn-Mn alloys for biomedical application [J]. Mater Sci Eng C, 2009, 29(3): 987−993.

[27] KIM H W, LEE S Y, BAE C J, NOH Y J, KIM H E. Porous ZrO_2 bone scaffold coated with hydroxyapatite with fluorapatite intermediate layer [J]. Biomaterials, 2003, 24(19): 3277−3284.

[28] WANG Yong, WEI Mei, GAO Jia-cheng. Improve corrosion resistance of magnesium in simulated body fluid by dicalcium phosphate dihydrate coating [J]. Mater Sci Eng C, 2009, 29(4): 1311−1316.

(Edited by LI Yan-hong)